3096 *Chem. Mater.* **2009,** *21,* 3096–3101
DOI:10.1021/cm9001064

CHEMISTRY OF MATERIALS
Article

Atomic Layer Deposition of Lanthanum Stabilized Amorphous Hafnium Oxide Thin Films

Tuo Wang and John G. Ekerdt*

Department of Chemical Engineering, The University of Texas at Austin, Austin, Texas 78712

Received January 13, 2009. Revised Manuscript Received May 8, 2009

Hafnium dioxide deposited on n-Si(100) by atomic layer deposition (ALD) was incorporated with La_2O_3 to stabilize the amorphous phase during high-temperature annealing. The incorporation of La was achieved by depositing HfO_2 and La_2O_3 in different ALD cycles that likely produced a $HfO_2-HfLa_xO_y$ periodic structure. X-ray photoelectron spectroscopy compositional analysis shows that the Hf and La atomic percentage ratio can be controlled by varying the Hf and La ALD cycle ratios. Microstructure was determined with X-ray diffraction and cross-sectional transmission electron microscopy. The introduction of La increases the film crystallization temperature from 500 °C for a HfO_2 film to 800, 900, and 950 °C for 10 nm films containing 13% La (metal basis), 25% La, and 43% La, respectively. The results indicate that ALD incorporating La is a potential method to grow amorphous $HfO_2-La_2O_3$ high-κ dielectric thin films.

1. Introduction

As the microelectronic industry transitions from conventional SiO_2 to high-κ materials to avoid excessive gate leakage current in the gate dielectric, hafnium dioxide (HfO_2) has attracted considerable attention.[1,2] It is desirable that the gate material remains amorphous throughout the necessary processing treatments because the grain boundaries in polycrystalline gate dielectrics may serve as high-leakage paths.[1] Some as-grown films can be amorphous,[3,4] but HfO_2 readily crystallizes upon annealing. Not only does HfO_2 require a post deposition 450 °C densification anneal,[5] there is a high-temperature dopant activation anneal at ~1000 °C,[6] that results in polycrystalline films. The polymorphs have different dielectric constants, viz., tetragonal is ~70, cubic is ~29, and monoclinic is about ~16.[7] Different phases often coexist in polycrystalline films,[8] which leads to a spatially varying dielectric constant. Zhao and Vanderbilt have shown that the dielectric constant varies by as much as 50% between different phases,[7] resulting in devices with variable capacitance values among different regions. Therefore, although crystalline HfO_2 has a higher dielectric constant, it is desirable to find methods to stabilize its amorphous phase after annealing. The dielectric constant for amorphous HfO_2 varies from 13 to 20,[9,10] but one may expect that it is close to that for the lowest-energy monoclinic crystalline phase.

To suppress crystallization, Al_2O_3 and SiO_2 have been incorporated into HfO_2.[11−13] Although $HfSiO_x$ and $HfAlO_x$ show higher crystallization temperatures than HfO_2, their dielectric constants decrease, reducing the advantage of the high-κ film. Another choice is La_2O_3, which is also a high-κ material, with a dielectric constant of more than 20.[14,15] Incorporating La into HfO_2 has been demonstrated as one method to stabilize an amorphous structure and one can expect this incorporation will not degrade the dielectric constant of the system because of the high-κ nature of La_2O_3. Lanthana incorporation has been reported using RF cosputtering and aqueous solution precipitation for the purpose of amorphous stabilization.[16,17] It is also reported that crystalline $La_2Hf_2O_7$

*Corresponding author. E-mail: ekerdt@che.utexas.edu. Tel.: (512) 471-4689. Fax: (512) 471-7060.

(1) Wilk, G. D.; Wallace, R. M.; Anthony, J. M *J. Appl. Phys.* **2001**, *89*, 5243–5275.
(2) International Technology Roadmap for Semiconductors, see www.itrs.net.
(3) Chiou, Y.-K.; Chang, C. -H.; Wu, T. -B. *J. Mater. Res.* **2007**, *22*, 1899–1906.
(4) Gusev, E. P.; Cabral, C.; Copel, M.; D'Emic, C.; Gribelyuk, M. *Microelectron. Eng.* **2003**, *69*, 145–151.
(5) Triyoso, D.; Liu, R.; Roan, D.; Ramon, M.; Edwards, N. V.; Gregory, R.; Werho, D.; Kulik, J.; Tam, G.; Irwin, E.; Wang, X.-D.; La, L. B.; Hobbs, C.; Garcia, R.; Baker, J.; White, B. E., Jr; Tobin, P. *J. Electrochem. Soc.* **2004**, *151*, F220–F227.
(6) Plummer, J. D.; Deal, M. D.; Griffin, P. B. Silicon VLSI Technology: Fundamentals Practice and Modeling; Prentice Hall: Upper Saddle River, NJ, 2000.
(7) Zhao, X.; Vanderbilt, D. *Phys. Rev. B* **2002**, *65*, 233106/1–233106/4.
(8) Mommer, N.; Lee, T.; Gardner, J. A. *J. Mater. Res.* **2000**, *15*, 377–381.
(9) Conley, J. F., Jr; Ono, Y.; Tweet, D. J.; Zhuang, W.; Solanki, R. *Mat. Res. Soc. Proc.* **2002**, *716*, 73–78.
(10) Kim, H.; Saraswat, K. C.; McIntyre, P. C. *J. Mater. Res.* **2005**, *20*, 3125–3132.
(11) Jones, A. C.; Aspinall, H. C.; Chalker, P. R.; Potter, R. J.; Manning, T. D.; Loo, Y. F.; O'Kane, R.; Gaskell, J. M.; Smith, L. M. *Chem. Vap. Deposit.* **2006**, *12*, 83–89.
(12) Wilk, G. D.; Wallace, R. M.; Anthony, J. M. *J. Appl. Phys.* **2000**, *87*, 484–492.
(13) Tomida, K.; Kita, K.; Toriumi, A. *Appl. Phys. Lett.* **2006**, *89*, 142902/1–142902/3.
(14) Guha, S.; Cartier, E.; Gribelyuk, M. A.; Bojarczuk, N. A.; Copel, M. C. *Appl. Phys. Lett.* **2000**, *77*, 2710–2712.
(15) Yeo, Y.-C.; King, T.-J.; Hu, C. *Appl. Phys. Lett.* **2002**, *81*, 2091–2093.
(16) Yamamoto, Y.; Kita, K.; Kyuno, K.; Toriumi, A. *Appl. Phys. Lett.* **2006**, *89*, 032903/1–032903/3.
(17) Ushakov, S. V.; Brown, C. E.; Navrotsky, A. *J. Mater. Res.* **2004**, *19*, 693–696.

Published on Web 06/29/2009

can be epitaxially grown on Si(001) by molecular beam epitaxy (MBE),[18] and pulsed laser deposition (LPD).[19]

Atomic layer deposition (ALD) is based on sequential, self-terminating surface reactions, which ensure atomic-level thickness control as the film grows linearly with the number of ALD cycles.[20] At present, ALD is one of the established techniques to grow amorphous as-deposited HfO_2 and La_2O_3 films.[21−25] In this paper, ALD is used to incorporate La in periodic $HfO_2-HfLa_xO_y$ structures, which are expected to be structurally different from sputtered homogeneous $HfLaO_x$ films and epitaxially grown $Hf_2La_2O_7$ or $HfO_2-La_2O_3$ bilayers.[26] ALD was first demonstrated in the 1970s.[27] The low growth rate for ALD is less of a problem for dielectric growth as ever thinner films are needed in complementary metal-oxide-semiconductor (CMOS) devices, and ALD has become an economically feasible method to grow highly conformal thin films for the semiconductor industry.

2. Experimental Section

The ALD system consists of a custom built, hot wall stainless steel vessel that is connected to a surface analysis chamber. Substrate samples are 2×2 cm^2 and are mounted on a molybdenum stage that can be moved in situ between the ALD chamber and the analysis chamber. The ALD chamber is pumped by a turbomolecular pump to a base pressure of 5×10^{-6} Torr and is connected to an X-ray photoelectron spectroscopy (XPS) analysis chamber through a load lock with a base pressure of 2×10^{-7} Torr. Films were deposited on n-Si(100) substrates at 250 °C using tetrakis (ethylmethylamino) hafnium $Hf[N(CH_3)(C_2H_5)]_4$, tris[N, N-bis(trimethylsilyl)-amino] lanthanum $La[N(SiMe_3)_2]_3$ and H_2O; the precursors were held at 85, 150, and 25 °C, respectively. The adsorption of $Hf[N(CH_3)(C_2H_5)]_4$ has been shown to be a self-limiting process at 250 °C.[21] The ALD of La_2O_3 using the same precursor is also reported at the same growth temperature,[23] although there might be a CVD component of the growth due to precursor decomposition.[28] To remove the native oxide from Si(100), we etched the Si substrates in a 2% HF solution for 30 s, rinsed in deionized water for 20 s, which reoxidized the Si(100) surface, and dried with flowing He. The resultant oxide is 10 Å according to spectroscopic ellipsometry (SE). All as-deposited samples were confirmed to be 11 nm (10 nm high-κ film + 1 nm SiO_2) by SE.

The incorporation of La was achieved by depositing HfO_2 and La_2O_3 in different cycles, and the La level was controlled by varying the ALD cycle ratio of the two oxides. One cycle consists of precursor dosing for 1.5 s, a 15 s purge with Ar, water dosing for 0.05 s, and a 25 s purge with Ar. The growth rate of HfO_2 and La_2O_3 in our ALD system is 0.78 Å/cycle and 0.50 Å/cycle, respectively. To deposit a film of a certain composition, we grow x cycles of HfO_2 plus one cycle of La_2O_3, and then repeat this sequence n times to achieve the desired thickness; films are referenced using $[x\text{Hf}+1\text{La}] \times n$. Note an ALD layer does not imply a complete monolayer of a particular material, and we refer to an ALD layer as the amount deposited in a single cycle. Film growth always ends with an xHf cycle to minimize adsorption of ambient CO_2 and H_2O on the La_2O_3.[29,30] Due to the layer-by-layer growth nature of ALD, we expect the $[x\text{Hf}+1\text{La}] \times n$ approach to lead to a periodic structure, with HfO_2 layers separated by $HfLa_xO_y$ layers.

X-ray photoelectron spectroscopy (XPS) with an Al $K\alpha$ source at 1486.6 eV was performed using a Physical Electronics 5500 XPS system to determine the film composition. A series of 10 nm films with different La incorporation levels (metal basis defined as La/(Hf+La)) was deposited by changing the HfO_2:La_2O_3 ALD cycle ratio from 1:1 to 8:1. After growth at 250 °C, samples were cooled to 70 °C in the ALD chamber and transferred to the XPS chamber through a load lock; the load lock is suspected of introducing some C contamination onto the sample surface since the load lock is repeatedly exposed to the ambient pressure when loading samples. Therefore, Ar^+ sputtering at 3 kV over a 3×3 mm^2 area for 90 s was performed to measure the atomic composition of the films. Approximately 3 nm is removed in this sputtering process.

To investigate the crystallinity of La incorporated HfO_2 films, grazing incidence X-ray diffraction (GIXRD) was performed at a fixed 0.5° incident angle, and 2θ scan rate of 6°/min. XRD was conducted with a Bruker-AXS D8 Advance Powder Diffractometer using a sealed tube Cu $K\alpha$ radiation. Prior to XRD, samples were annealed by rapid thermal annealing at different temperatures for 30 s under a N_2 ambient.

Cross-sectional high resolution transmission electron microscopy (HRTEM) images were obtained to examine the morphology and microstructure of the HfO_2 films at different incorporation levels and different annealing temperatures. The cross sections were prepared using a dicing saw followed by focused ion beam (FIB) milling. The FIB milling was conducted with a FEI Strata DB235 dual beam SEM/FIB system, which combines a scanning electron microscope (SEM) with a Ga ion beam source for nanoscale cutting. The thinning process starts at a rough milling step under 3000 pA, followed by a fine milling step under 300 pA, and finally a cleaning cross-section milling step under 30 pA. TEM images were acquired using a JEOL 2010F high-resolution transmission electron microscope with a field emission gun operated at 200 kV.

For preliminary electrical measurements concerning film dielectric constant, metal−insulator−semiconductor (MIS) capacitors were made by depositing TaN using DC sputtering. The area of TaN contact was defined by a shadow mask, and measured with a Zeiss Axioskop 2 MAT optical microscope.

(18) Dimoulas, A.; Vellianitis, G.; Mavrou, G.; Apostolopoulos, G.; Travlos, A.; Wiemer, C.; Fanciulli, M.; Rittersma, Z. M. *Appl. Phys. Lett*. **2004**, *85*, 3205–3207.
(19) Wei, F.; Tu, H.; Wang, Y.; Yue, S.; Du, J. *Appl. Phys. Lett*. **2008**, *92*, 012901/1–012901/3.
(20) Suntola, T. *Thin Solid Films* **1992**, *216*, 84–89.
(21) Kukli, K.; Ritala, M.; Sajavaara, T.; Keinonen, J.; Leskela, M. *Chem. Vap. Deposition* **2002**, *8*, 199–204.
(22) Hausmann, D. M.; Kim, E.; Becker, J.; Gordon, R. G. *Chem. Mater*. **2002**, *14*, 4350–4358.
(23) He, W.; Schuetz, S.; Solanki, R.; Belot, J.; McAndrew *J. Electrochem. Solid-State Lett*. **2004**, *7*, G131–G133.
(24) Triyoso, D. H.; Hegde, R. I.; Grant, J.; Fejes, P.; Liu, R.; Roan, D.; Ramon, M.; Werho, D.; Rai, R.; La, L. B.; Baker, J.; Garza, C.; Guenther, T.; White, B. E., Jr; Tobin, P. J *J. Vac. Sci. Technol., B* **2004**, *22*, 2121–2127.
(25) Kukli, K.; Ritala, M.; Pore, V.; Leskela, M.; Sajavaara, T.; Hegde, R. I.; Gilmer, D. C.; Tobin, P. J.; Jones, A. C.; Aspinall, H. C. *Chem. Vap. Deposition* **2006**, *12*, 158–164.
(26) Mavrou, G.; Galata, S.; Tsipas, P.; Sotiropoulos, A.; Panayiotatos, Y.; Dimoulas, A.; Evangelou, E. K.; Seo, J. W.; Dieker, Ch *J. Appl. Phys*. **2008**, *103*, 014506/1–014506/9.
(27) Suntola, T.; Antson, A. US Pat. 4058430 (**1977**).
(28) Jones, A. C.; Aspinall, H. C.; Chalker, P. R.; Potter, R. J.; Kukli, K.; Rahtu, A.; Ritala, M.; Leskelae, M. *Mater. Sci. Eng., B* **2005**, *118*, 97–104.
(29) Suzuki, M.; Kagawa, M.; Syono, Y.; Hirai, T. *J. Cryst. Growth* **1991**, *112*, 621–627.
(30) De Asha, A. M.; Critchley, J. T. S.; Nix, R. M. *Surf. Sci*. **1998**, *405*, 201–214.

The capacitance−voltage ($C-V$) characteristics were measured using a Keithley 590 CV Analyzer controlled by a Keithley 4200 Semiconductor Characterization System.

3. Results and Discussion

A. Compositional Analysis. Figure 1 shows the X-ray photoelectron spectra for La 2p, Si 2s, and Hf 4f of the as-deposited films. As the La incorporation level increases (smaller x in $[x\text{Hf}+1\text{La}]\times n$), the La 2p peak intensity increases along with a corresponding decrease in the Hf 4f peak intensity, indicating La has been successfully incorporated into the films. The major impurity is Si from the La precursor, which is commonly observed in ALD grown La_2O_3 using the same precursor.[31] The Si 2s signal is shown instead of the more common Si 2p signal because the latter overlaps with the La 4d peak. The intensity of Si 2s increases simultaneously with increasing La incorporation level. The peak positions for these three elements do not show any shifts with respect to different La incorporation level. A very weak N 1s feature appears at 389 eV (not shown), which comes from the Hf precursor. No peak was found for C 1s at 285 eV (not shown) in the films, indicating any C impurities are below the XPS detection limits ($<1\%$) in the bulk film after sputtering off the topmost surface. The Hf $4f_{7/2}$ peak appears at 18.5 eV, indicating the formation of Hf−O bonding and the Hf^{4+} oxidation state in the bulk film.[32] The La $3d_{5/2}$ core level appears at 836.9 eV, consistent with La_2O_3 or La silicate.[33] The O 1s state appears at 532.1 eV for all La incorporation levels (bottom inset of Figure 2). Considering that the O 1s state of HfO_2 films appears at 532 eV (not shown) in our XPS system, the incorporation of La does not affect the Hf−O bonding significantly.

The as-deposited film atomic composition is calculated from the integrated photoemission intensities corrected by their atomic sensitivity factors.[34] The Hf and La atomic concentrations are shown in the top inset of Figure 2 and the main plot presents the La incorporation level on a Si-free metal basis. Figure 2 illustrates the La incorporation level in HfO_2 can be well-controlled by varying the ALD growth cycles of the two oxides. The highest La incorporation level of 43% was reached for one deposition cycle of HfO_2 followed by one cycle of La_2O_3, i.e., [1Hf+1La]. At this nominal 50:50 condition, the film contains more Hf than La because the ligands on the La precursor are larger than on the Hf precursor, and the greater steric hindrance can reduce the number of precursor molecules absorbed with every La dosing cycle.

B. Crystallinity and Dielectric Constant. The XRD patterns in Figure 3 show that the temperature for the onset of crystallization increases as the La incorporation level increases. Others have reported that 10 nm HfO_2 films crystallize at 500 °C,[4] and we obtained the same result, as shown in the inset of Figure 3. By adding one cycle of La_2O_3 after every six cycles of HfO_2 (La/(Hf+La)=13%), the 10 nm thin film remains amorphous after 800 °C annealing. Increasing the La incorporation level by depositing one cycle of La_2O_3 after every three cycles of HfO_2 (La/(Hf+La) = 25%) enables the 10 nm

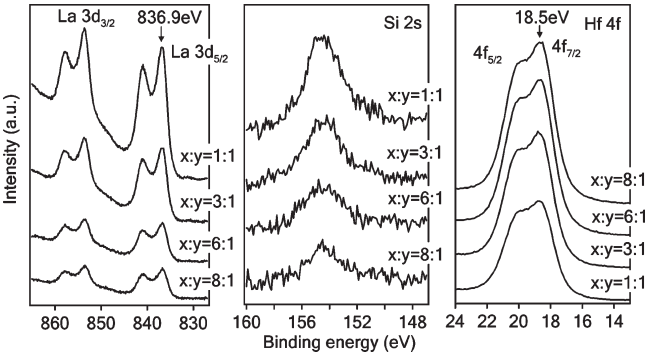

Figure 1. XP spectra of La 3d, Si 2p, and Hf 4f at different La incorporation levels. The x:y designations refer to the HfO_2:La_2O_3 ALD cycle ratios.

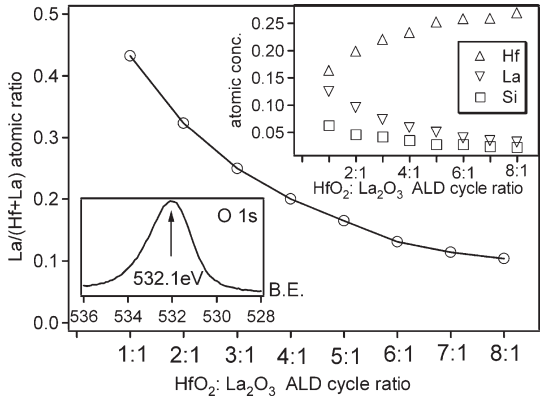

Figure 2. Hf, La, and Si atomic concentration (top inset) and La doping level (metal based) as a function of HfO_2:La_2O_3 ALD cycle ratio; bottom inset, O 1s peak for all La incorporation levels.

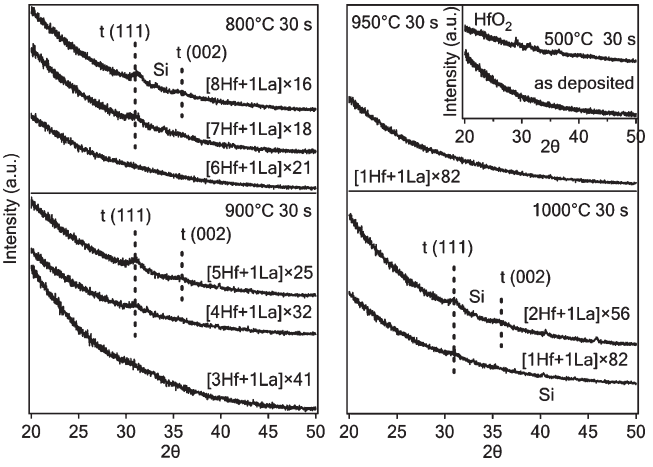

Figure 3. XRD spectra of 10 nm $HfLa_xO_y$ films after 30 s annealing in a N_2 ambient; inset, XRD spectra for 10 nm HfO_2.

(31) Triyoso, D. H.; Hegde, R. I.; Grant, J. M.; Schaeffer, J. K.; Roan, D.; White, B. E., Jr; Tobin, P. J. *J. Vac. Sci. Technol., B* **2005**, *23*, 288–297.
(32) Lay, T. S.; Chang, S. C.; Din, G. J.; Yeh, C. C.; Hung, W. H.; Lee, W. G.; Kwo, J.; Hong, M. *J. Vac. Sci. Technol., B* **2005**, *23*, 1291–1293.
(33) Copel, M.; Cartier, E.; Ross, F. M. *Appl. Phys. Lett.* **2001**, *78*, 1607–1609.
(34) Moulder, J. F.; Stickle, W. F.; Sobol, P. E.; Bomben, K. D. Handbook of X-ray Photoelectron Spectroscopy; Physical Electronics, Inc.: Eden Prairie, MN, 1995.

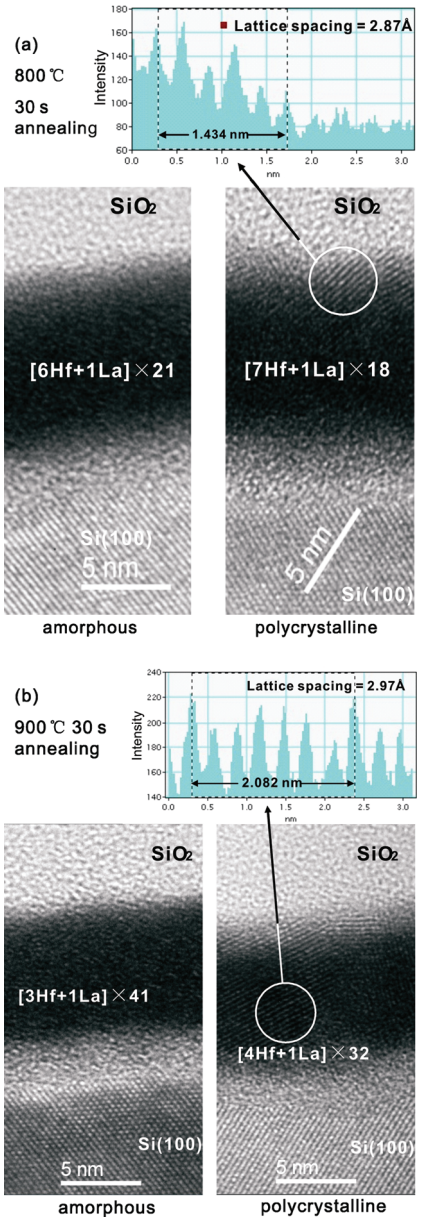

Figure 4. Cross-sectional HRTEM images for samples above and below the La incorporation levels that stabilize an amorphous structure at (a) 800 and (b) 900 °C.

amorphous film to withstand 900 °C annealing. When HfO_2:La_2O_3=1:1, a 10 nm amorphous film can withstand 950 °C annealing, but becomes crystallized after 1000 °C annealing. Because only two peaks are detected in the 10 nm films, it is difficult to distinguish between monoclinic and tetragonal phases. The peaks after crystallization occur at $2\theta = 31$ and 36°. These two peaks are close to tetragonal (111) and tetragonal (002) for HfO_2.[35] The calculated d spacing is 2.97 Å for t(111), and 2.62 Å for t(002).

The HRTEM images in Figure 4 show the representative samples at La incorporation levels necessary to keep the films amorphous at 800 and 900 °C and just below those La incorporation levels. The total oxide thickness

(35) Powder Diffraction File PDF 08−0342; International Center for Diffraction Data: Newtown Square, PA, **2001**.

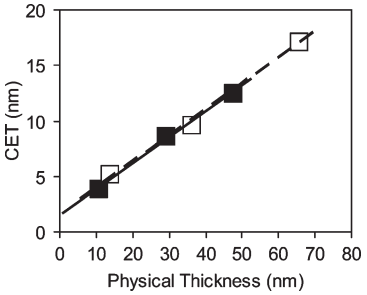

Figure 5. CET as a function of physical thickness (measured by SE). HfO_2 films (□) were annealed at 500 °C for 30 s, and [6Hf+1La] films (■) were annealed at 800 °C for 30 s. The fits for HfO_2 (dash line) and [6Hf+1La] (solid line) lead to κ of 16.7 ± 0.3 and 16.6 ± 0.4, respectively.

(interfacial SiO_2 + $HfLa_xO_y$) is 11 nm for each sample, consistent with thicknesses predicted by SE. In terms of crystallinity, while a 10 nm [6Hf+1La] film remains completely amorphous after 800 °C annealing, adding an extra HfO_2 layer leads to a partially crystallized film after annealing at the same temperature (Figure 4a). Similarly, a [4Hf+1La] film changed into a polycrystalline film after annealing at 900 °C, but a [3Hf+1La] film was still amorphous after annealing at 900 °C (Figure 4b). The random orientations of the lattice fringes in the crystallized samples (Figure 4) illustrate that the films were polycrystalline. The lattice spacing within the highlighted region is 2.87 Å for the [7Hf+1La] film, and 2.97 Å for the [4Hf+1La] film. These results are consistent with XRD results in Figure 3 where the d spacing for t(111) is 2.97 Å.

To measure the dielectric constant, MIS capacitors were made. The typical 100 kHz C−V measurements were performed for HfO_2 annealed at 500 °C and 13% La-incorporated [6Hf+1La] × n films annealed at 800 °C. 500 and 800 °C were chosen because at these temperatures HfO_2 films became polycrystalline while [6Hf+1La] films remained amorphous, which serves to illustrate the comparison between a polycrystalline gate dielectric and an amorphous dielectric that could form under annealing temperatures that mimic the real device fabrication process. The dielectric constant was determined from the slope of capacitance equivalent thickness (CET) versus physical thickness curves, where CET was measured at $V_g = -5$ V of the accumulation capacitance of the $C-V$ curves and physical thickness was measured by SE. From linear fitting in Figure 5, HfO_2 films have a dielectric constant of 16.7 ± 0.3, and 13% La-incorporated [6Hf+1La]×n films have a dielectric constant of 16.6 ± 0.4, indicating that La incorporation did not degrade the film in terms of dielectric constant.

C. Evidence of a Periodic Structure and Its Comparison to Homogeneous Films. Due to the ALD growth mechanism, we expect a periodic film structure composed of repeated $HfLa_xO_y$ layers separated by HfO_2 layers is formed. To verify the existence of periodicity, we performed angle-resolved XPS at small take off angles (angles between sample surface and photoelectron detector) to investigate the topmost overlayers of films. At smaller XPS take off angles, photoelectrons are detected

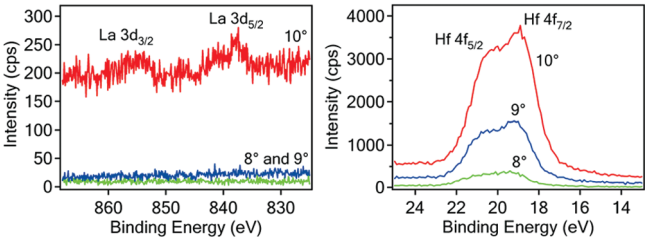

Figure 6. XP spectra of La 3d and Hf 4f spectra of a 10 nm [6Hf+1La] × 21 sample at take off angle = 8, 9, and 10°.

Table 1. Comparison of Lowest La Incorporation Concentration (metal based) that ALD Periodic Structure and Homogeneous Films Require to Suppress Crystallization after 800 and 900 °C Annealing

annealing temperate (°C)	ALD periodic structure films (%)	homogeneous films[16] (%)
800	13 ([6Hf+1La] film)	20
900	25 ([3Hf+1La] film)	40

shallower in the film overlayer. Figure 6 shows the in situ La 3d and Hf 4f XPS spectra of an as-deposited 10 nm [6Hf+1La] × 21 sample without Ar^+ sputtering at take off angles of 8, 9, and 10°. The unit of intensity is in counts per second (cps) so that the absolute values of the peak intensity can be compared. While the Hf peak gradually increases with increasing XPS take off angle, the La peak abruptly shows up at 10°. The absence of La peaks for take off angles smaller than 10° indicates the existence of a top La free overlayer wholly composed of HfO_2, and an underlying $HfLa_xO_y$ layer corresponding to the La signal when the detection overlayer is deeper than a certain thickness. Therefore, we conclude the existence of a top HfO_2−$HfLa_xO_y$ structure, resulting from the last [6Hf+1La] ALD sequence, which is different from a homogeneous HfO_2−La_2O_3 mixture. Although is difficult to characterize the bulk film using the same technique, we believe this film is composed of 21 similar HfO_2−$HfLa_xO_y$ structures because of the layer-by-layer growth nature of ALD.

Table 1 lists a comparison of the amorphous stabilization effects between 10 nm ALD periodic structure films in this study and 30 nm homogeneous films grown by RF cosputtering in ref 16. Periodic structure films appear to require lower La incorporation levels to stabilize the amorphous structure. Overall film thickness can be a contributing factor to amorphous film stabilization. To investigate the impact of overall film thickness in ALD-grown films, we deposited four films (3, 10, 30, and 50 nm) at a constant 13% La incorporation level, i.e., [6Hf + 1La]. As shown in Figure 7, all four films remained amorphous after 800 °C annealing, and only the ultrathin, 3 nm film remained amorphous after annealing at 1000 °C. The Si atomic concentration for a [6Hf+1La] film and a [3Hf+1La] film in this study is 2.4 and 3.5%, respectively. The Si impurities may be an additional contributing factor in the stabilization of our films. However, in separate studies a Si incorporation level of 10% was unable to stabilize the amorphous phase after 800 °C annealing.[13]

The results reported herein illustrate how both the amount of La incorporated and its location in the film

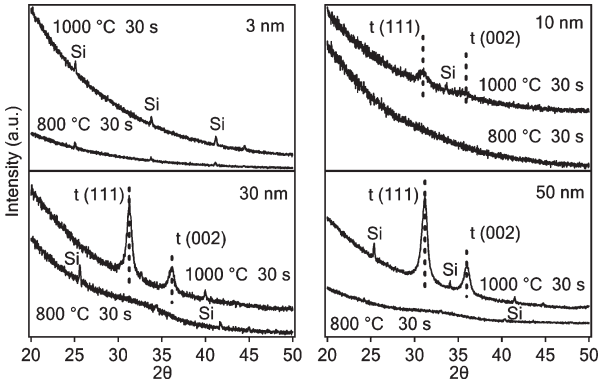

Figure 7. XRD spectra of [6Hf+1La] films of different thickness (3, 10, 30, and 50 nm) after 800 and 1000 °C annealing under a N_2 ambient for 30 s.

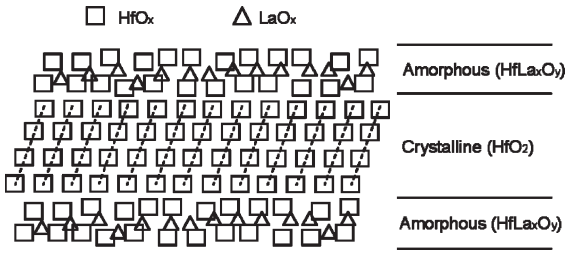

Figure 8. Pictorial presentation of the periodic structure during the intermediate state of the crystallization process.

affect its ability to stabilize the amorphous phase. A possible reason for this location effect might be the formation of the HfO_2−$HfLa_xO_y$ periodic structure formed by repeatedly adding one ALD layer of La_2O_3 on *n* layers of HfO_2. As temperature is elevated, the HfO_2 between $HfLa_xO_y$ layers is expected to crystallize first while the $HfLa_xO_y$ layers would remain amorphous in the same way as homogeneous $HfLa_xO_y$ films with a high La incorporation concentration remain amorphous. This interpretation is illustrated in Figure 8. If crystals are nucleated within HfO_2, the film has to overcome an extra energy barrier compared to pure homogeneous HfO_2, because of the interfaces between crystallized HfO_2 and amorphous $HfLa_xO_y$ layers.

Furthermore, we may expect that the crystallization onset temperature is essentially determined by the thickness of the HfO_2 region between the $HfLa_xO_y$ layers. In this amorphous stabilization model, a lower HfO_2:La_2O_3 ALD cycle ratio (smaller *x* in [*x*Hf+1La]×*n*) does not increase the local La atomic concentration in the $HfLa_xO_y$ layers, but does decrease the thickness of HfO_2 interval layers. The La atomic concentration in the $HfLa_xO_y$ layer should remain constant and behave in the same way as homogeneous $HfLa_xO_y$ films. The thinner HfO_2 interval layers themselves can withstand higher annealing temperature due to their higher surface-to-volume ratio because amorphous oxide is found to have the smallest surface enthalpy.[36] For thinner HfO_2 layers, the increase in surface enthalpy upon crystallization would be large enough to make the amorphous phase more stable even though the crystalline phase is more thermodynamically

(36) Navrotsky, A. *J. Mater. Chem.* **2005**, *15*, 1883–1890.

favored in bulk films. Therefore, the amorphous stabilization mechanism(s) for homogeneous and ALD periodic structure films can be very different, although both are enhanced by adding more La.

4. Conclusion

In summary, La has been successfully incorporated into HfO_2 using ALD. XPS analysis shows that the La incorporation level was effectively controlled by varying the HfO_2:La_2O_3 ALD cycle ratio. XRD and cross-sectional HRTEM show that the crystallization temperatures for La-incorporated HfO_2 films have been increased significantly. A 10 nm [6Hf+1La] × 21 (La/(Hf+La) = 13%) film remains amorphous after 800 °C annealing, a 10 nm [3Hf+1La] × 41 (La/(Hf+La) = 25%) film remains amorphous after 900 °C annealing, and a 10 nm [1Hf+1La] ×82 (La/(Hf+La) = 43%) film remains amorphous after 950 °C annealing. The film dielectric constant was not degraded after La incorporation. The ALD grown films require a lower La incorporation level to sustain a certain annealing temperature compared with homogeneous films, probably because a layered HfO_2−$HfLa_xO_y$ periodic structure is formed. Incorporating La into HfO_2 using ALD is a potential method to fabricate high-κ dielectric gate materials for future CMOS devices.

Acknowledgment. This work was supported by the National Science Foundation (Awards DMR-060646 and NNIN ECS-0335765).